ORNL-TM-2836

Contract No. W-7405-eng-26

METALS AND CERAMICS DIVISION

PENETRATION OF REFRACTORY METALS BY ALKALI METALS

R. L. Klueh

APRIL 1970

OAK RIDGE NATIONAL LABORATORY
Oak Ridge, Tennessee
operated by
UNION CARBIDE CORPORATION
for the
U.S. ATOMIC ENERGY COMMISSION

CONTENTS

PENETRATION OF REFRACTORY METALS BY ALKALI METALS

R. L. Klueh

ABSTRACT

Under certain conditions liquid alkali metals penetrate tantalum and niobium rapidly along grain boundaries and certain crystallographic planes. Penetration is observed only when oxygen dissolved in the refractory metal exceeds some threshold concentration, which depends upon the refractory metal, the alkali metal, and the temperature. Penetration was first encountered in niobium and tantalum exposed to lithium, but has now been found when these metals are exposed to sodium, potassium, and the sodium-potassium eutectic. Oxygen levels required to effect penetration in niobium and tantalum by lithium, sodium, and potassium at 600°C are compared, and the rate of penetration is discussed in terms of a corrosion model.

INTRODUCTION

Liquid metals are attractive as heat transfer and working fluids for nuclear reactors, and for the past 20 years much work has been directed at determining the compatibility of liquid metals with structural and container materials. In recent years the liquid metals of most interest have been the alkali metals lithium, sodium, and potassium. For containment at high temperatures, the refractory metals – niobium, tantalum, molybdenum, and their alloys – show considerable promise.

Refractory metals are resistant to alkali metal corrosion when the system contains no impurities – especially oxygen. The effect of oxygen on compatibility differs depending upon whether the oxygen is in the alkali metal or the refractory metal. An increase in the oxygen concentration of the alkali metal may lead to increased dissolution of the refractory metal, as we recently showed for the niobium-sodium[1] and niobium-potassium[2] systems. Oxygen in the refractory metal, on the other hand, may lead to severe penetration of the refractory metal by the alkali metal. This latter effect will be discussed here.

BLANK PAGE

Oxygen-induced alkali metal penetration was first detected in the niobium-lithium system, and this system was studied by a number of investigators.[3–6] The important features of the penetration process can be characterized as follows.

1. The oxygen concentration of niobium must exceed a "threshold level" before lithium penetrates. The threshold oxygen concentration increases with temperature. Penetration is independent of the oxygen concentration in the lithium.

2. Botn intergranular (grain boundary) and transgranular (with a {110} habit plane) attack occur, as shown in Fig. 1. The threshold for intergranular attack is less than that for transgranular attack.

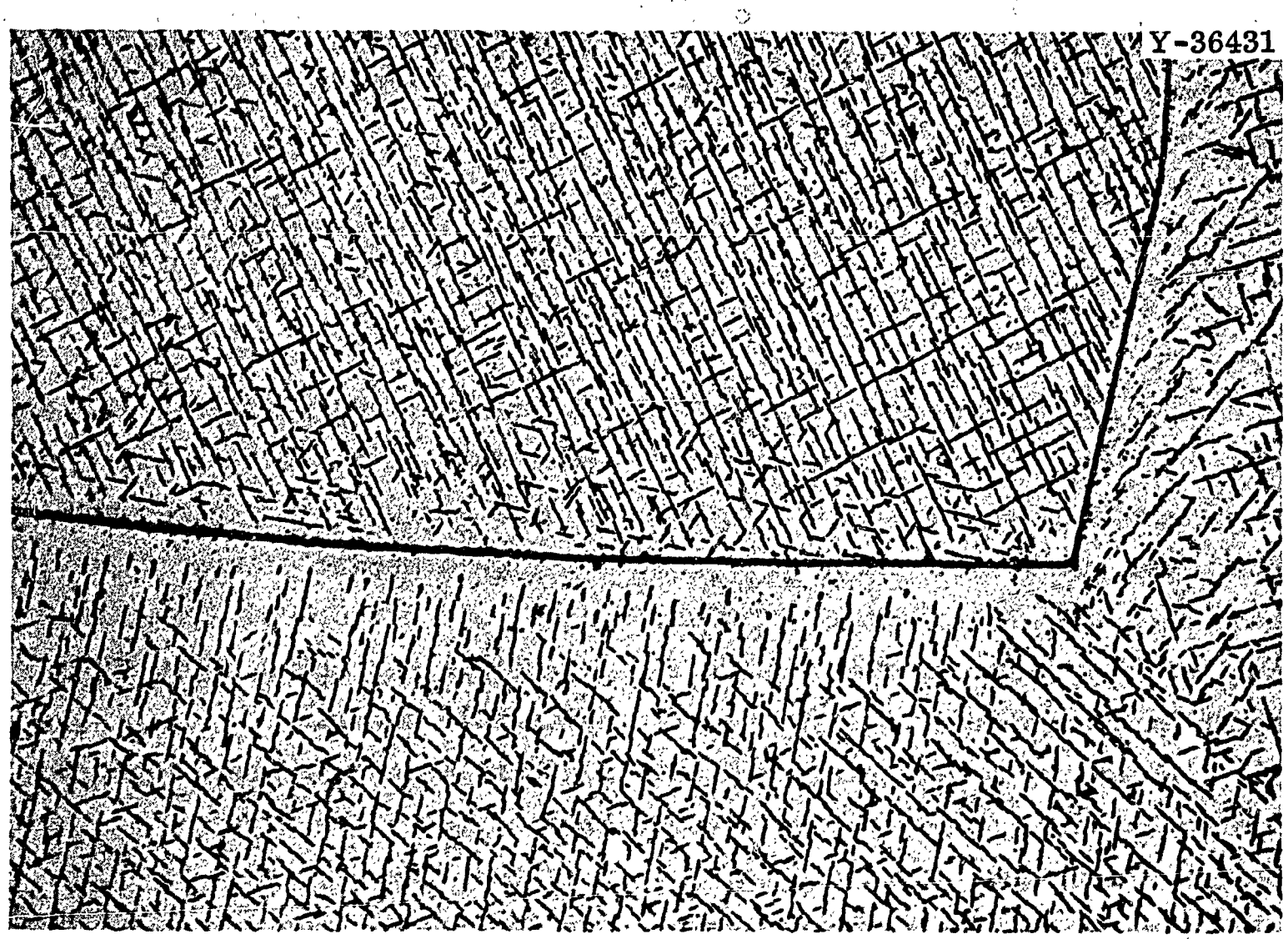

Fig. 1. Intergranular and Transgranular Penetration of Niobium Containing 1500 ppm O and Exposed to Lithium for 100 hr at 816°C. 750×. Etchant: $HF-HNO_3-H_2SO_4-H_2O$. [Ref: J. R. DiStefano, Corrosion of Refractory Metals by Lithium, ORNL-3551 (March 1964).]

3. Lithium attack is extremely rapid; DiStefano[5] reports that a 0.040-in. specimen with 1900 ppm O was completely penetrated at 1100°C in 0.5 hr, and a 0.040-in. single-crystal specimen with about 4000 ppm O was completely penetrated at 815°C in 1 hr. The rate increases with increasing oxygen concentration in the niobium.[6]

4. Not all specimens are completely penetrated even after long exposure times. The depth of attack increases with increasing oxygen in the niobium, and for a given oxygen level in the niobium, the depth of transgranular attack goes through a maximum at 600°C (ref. 5).

Penetrated niobium showed increased lithium and decreased oxygen concentrations. Metallography showed the presence of a corrosion product in the penetrated specimens, and an x-ray diffraction pattern obtained from the corrosion product was different from that for Li_2O. It appears, therefore, that lithium penetration results from the formation of a product containing lithium, niobium, and oxygen (i.e., a niobate, although the diffraction patterns of the corrosion product could not be successfully matched to any lithium niobate patterns[5]).

DiStefano[5] also observed the lithium attack of oxygen-doped tantalum. Oxygen-induced attack of niobium and tantalum by sodium, potassium, and the sodium-potassium eutectic, NaK, has also been observed. Some recent experiments at Oak Ridge National Laboratory[7] that employed unalloyed tantalum thermocouple tube sheaths in contact with NaK failed in less than 5 hr at 250 to 300°C when the NaK penetrated the 0.007-in. sheath wall. Harrison[8] showed that tantalum specimens containing more than 270 ppm O were attacked by NaK at 650 and 730°C. Litman[9] found that niobium containing more than 1000 and 1300 ppm O is intergranularly attacked at 600 and 800°C, respectively, and Hickam[10] observed the penetration of tantalum by potassium.

The problem of lithium penetration of niobium was circumvented by the addition of small amounts of zirconium (at least 1%) to the niobium.[4,5] Zirconium reacts with the oxygen dissolved in the metal to form ZrO_2, thereby lowering the chemical activity of oxygen in solid solution. Tantalum is similarly rendered more resistant to lithium attack by the addition of hafnium.[11]

Although the problem of penetration has been reduced by the development of more corrosion-resistant alloys, the mechanism of penetration is

still not clear. The purpose of the present studies, therefore, was to gain insight into the penetration process.

EXPERIMENTAL PROCEDURE

Oxygen was added to niobium and tantalum test specimens of 99.9% purity by annealing at 1000°C in an oxygen pressure of 1×10^{-4} torr in a vacuum system with a controlled oxygen leak. After oxidation the specimens were vacuum homogenized at 1400°C for 4 hr; homogenization was checked by microhardness measurements. Before and after exposure to the liquid metal the oxygen concentration was determined by either vacuum-fusion or fast-neutron activation analysis.

The specimens were exposed to alkali metals either singly or in groups in capsules of the type shown schematically in Fig. 2. The

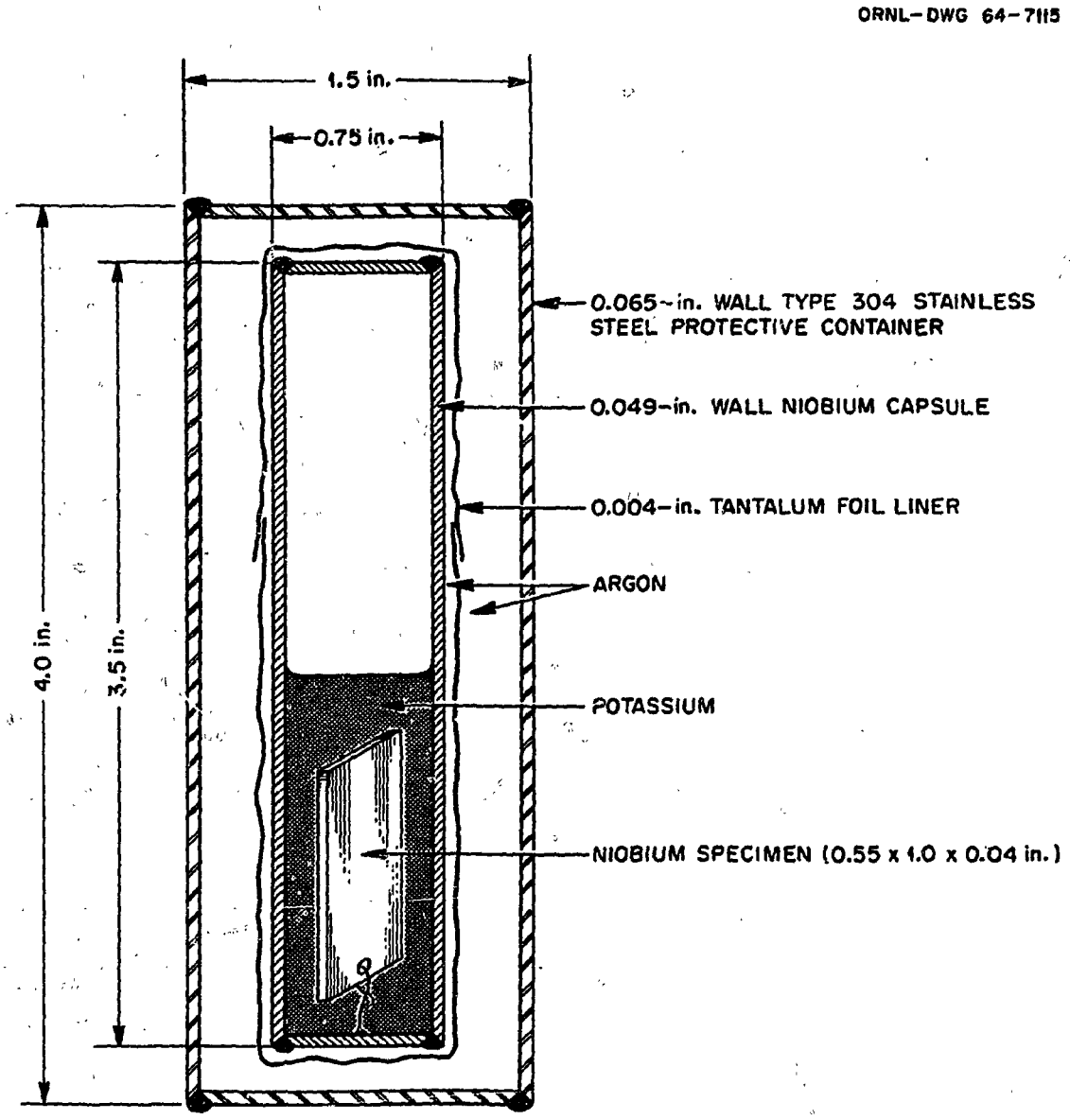

Fig. 2. Schematic Diagram of Test System.

alkali metals were purified to ≥ 99.8% by exposure to zirconium foil before test. The capsules were loaded and welded in an argon-filled chamber to prevent contamination of the alkali metal or refractory metal. A stainless steel outer container protected the capsules from air oxidation during test, and a tantalum foil wrap protected the capsules against impurities from the stainless steel. While being heated to the test temperature, the specimens were in the vapor zone, and when the system reached temperature the capsule was inverted to immerse the specimen in the liquid.

After test the capsules were inverted, quenched in liquid nitrogen, and opened in the argon chamber, and the alkali metal was removed by dissolving in chilled isopropyl alcohol. The specimens were examined metallographically to determine the extent of penetration.

RESULTS

Comparison of Systems

The behavior of oxygen-doped tantalum and niobium in potassium, sodium, and lithium was compared at 600°C. To estimate the minimum or "threshold" oxygen concentration in the refractory metal required to induce penetration, a series of specimens with different oxygen concentrations was examined metallographically after test. The results are given in Table 1. The threshold concentration was highest for potassium and lowest for lithium, and the threshold concentration for tantalum was about half that for niobium (on a weight basis).

Figure 3 shows tantalum specimens that contained about 1300 ppm* of dissolved oxygen after exposure to potassium, sodium, and lithium. Similar unexposed specimens showed no evidence of precipitate. The amount of attack for a given oxygen concentration was least for potassium and most for lithium.

Decreasing the oxygen concentration of the tantalum decreased both the depth of attack and the number of grain boundaries attacked. Figure 4

---

*All concentrations are in parts per million by weight.

Table 1. Estimated Threshold Oxygen Concentrations in Refractory Metals for Grain-Boundary Penetration by Alkali Metals at 600°C

Refractory Metal	Threshold Oxygen Concentration (ppm by weight)		
	Potassium	Sodium	Lithium
Tantalum	500	300	150
Niobium	1000	800	400

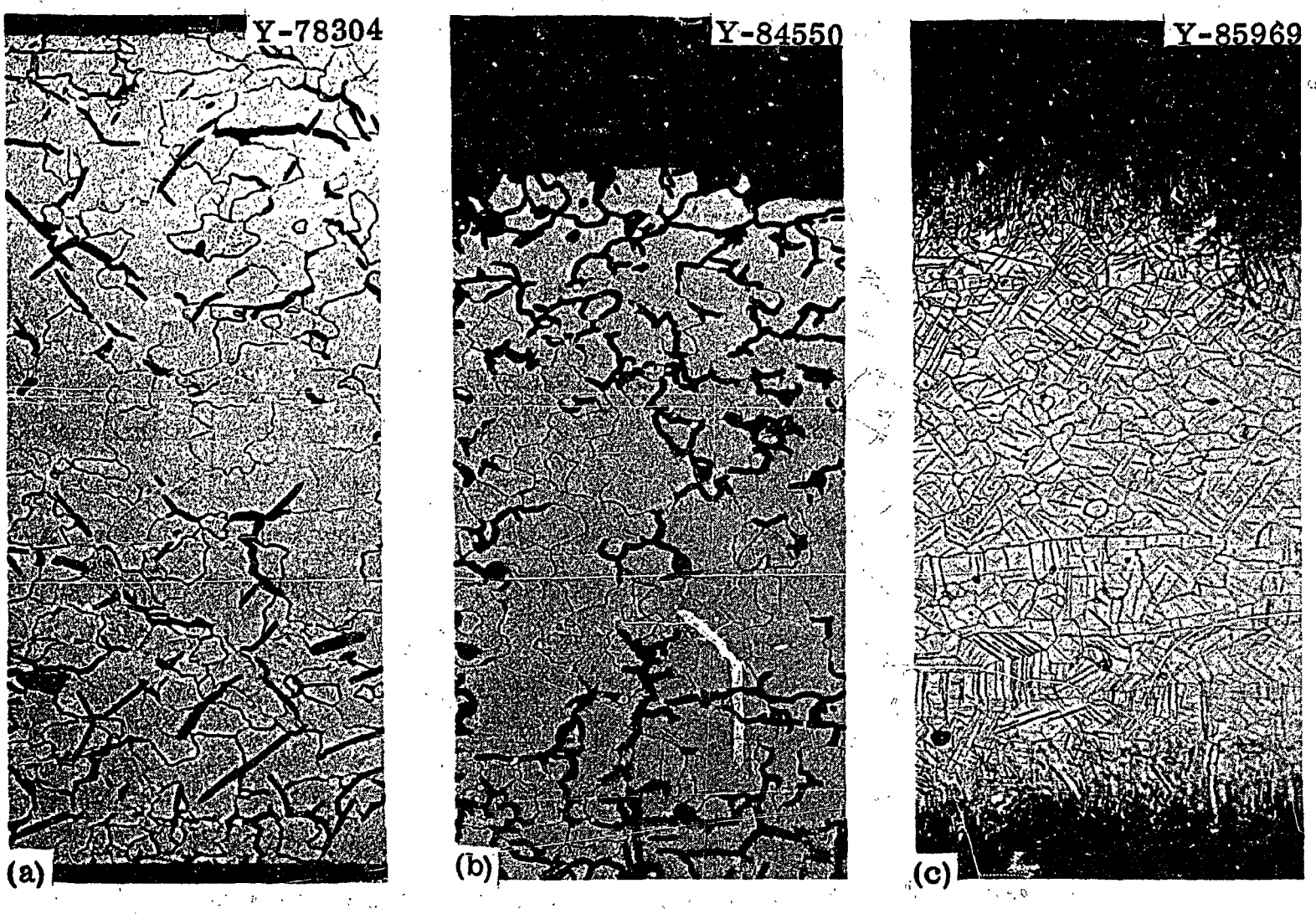

Fig. 3. Tantalum Specimens Exposed to Alkali Metals for 500 hr at 600°C. 100×. Etchant: H_2O-HNO_3-NH_4HF. (a) Initially 1300 ppm O; exposed to potassium. (b) Initially 1400 ppm O; exposed to sodium. (c) Initially 1200 ppm O; exposed to lithium.

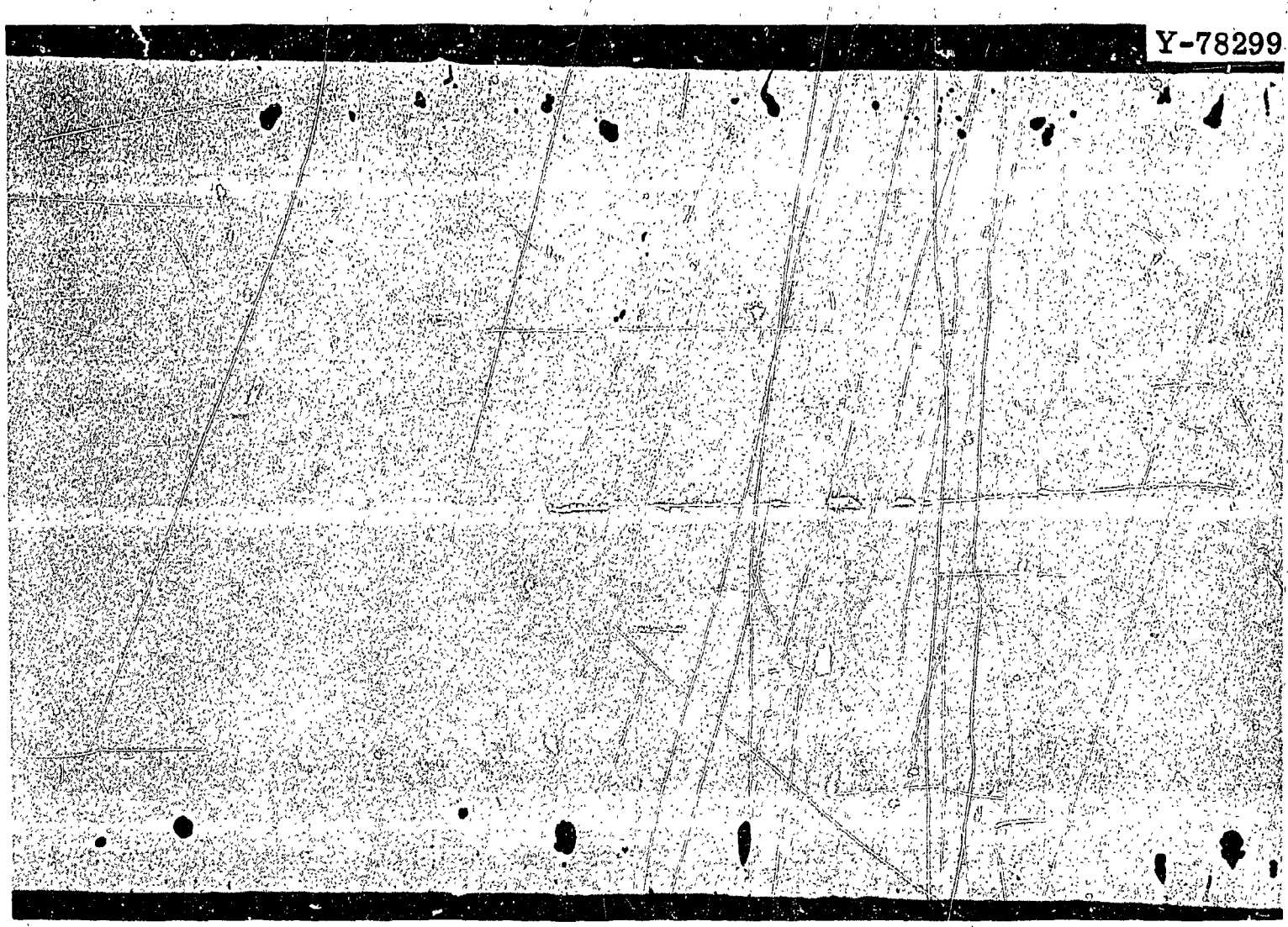

Fig. 4. Tantalum That Contained 600 ppm O and Was Exposed to Potassium for 500 hr at 600°C. The 0.002- to 0.004-in.-deep dark areas are corrosion pockets or "heads" that terminate attack along grain boundaries. 100×. Unetched.

shows a tantalum specimen that contained 600 ppm O and was exposed to potassium at 600°C. This specimen illustrates the type of attack that occurs at or just above the threshold oxygen concentration. The attack is completely intergranular (as revealed by etching) and terminates in relatively large corrosion pockets or penetration "heads."

The high susceptibility of tantalum to lithium attack is demonstrat by the observations on the capsules used in these experiments. When the tantalum capsules were removed from the stainless steel outer containers they were discolored and appeared to have leaked during test. Since no weld or other failures were apparent, we concluded that although the tantalum contained only about 200 ppm O, the lithium penetrated the 0.062-in. walls. This was confirmed when the tube walls were sectioned and examined metallographically, as shown by Fig. 5.

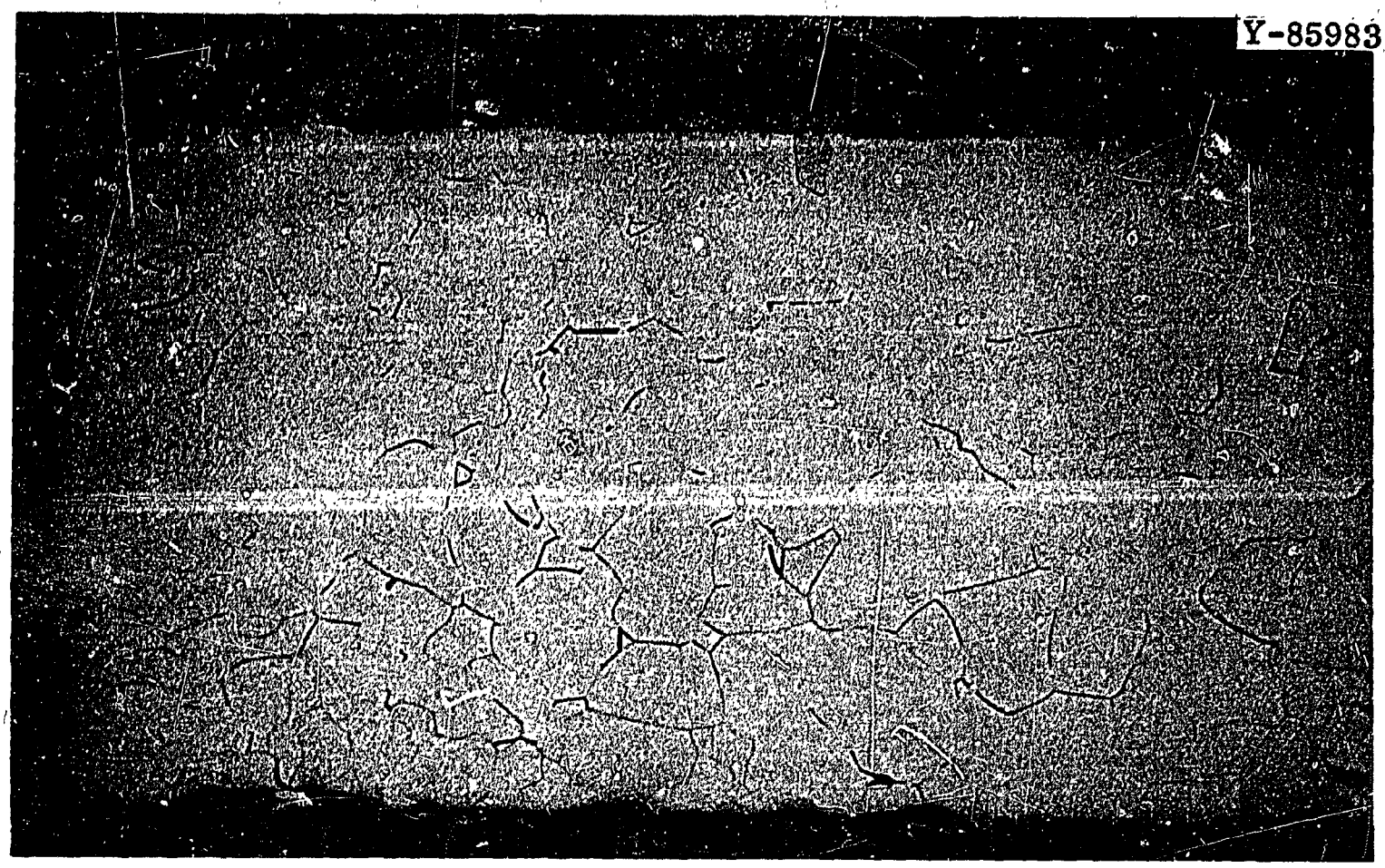

Fig. 5. Tantalum Tubing That Contained 200 ppm O and Was Exposed to Lithium for 500 hr at 600°C. 50×. Etchant: H_2O-HNO_3-NH_4HF.

Figure 6 shows a niobium specimen that contained about 2200 ppm O before lithium exposure at 600°C. The difference between niobium and tantalum is seen by comparing Figs. 3(c) and 6. Although the niobium specimen with 2200 ppm O was completely penetrated intergranularly, transgranular penetration was incomplete. However, tantalum with only 1200 ppm O was completely penetrated by both modes.

Effect of Temperature

Tantalum specimens were exposed to potassium at 600, 800, and 1000°C to determine how temperature affects the threshold oxygen concentration for penetration. Figure 7 compares tantalum specimens that initially contained 1200 and 700 ppm O after exposure at 800°C. These photomicrographs should be compared with Figs. 3(a) and 4, which show tantalum specimens predoped to similar oxygen levels but exposed at 600°C. Penetration is much more severe at the lower temperature. In fact when a tantalum specimen containing 700 ppm O was exposed to potassium at 1000°C,

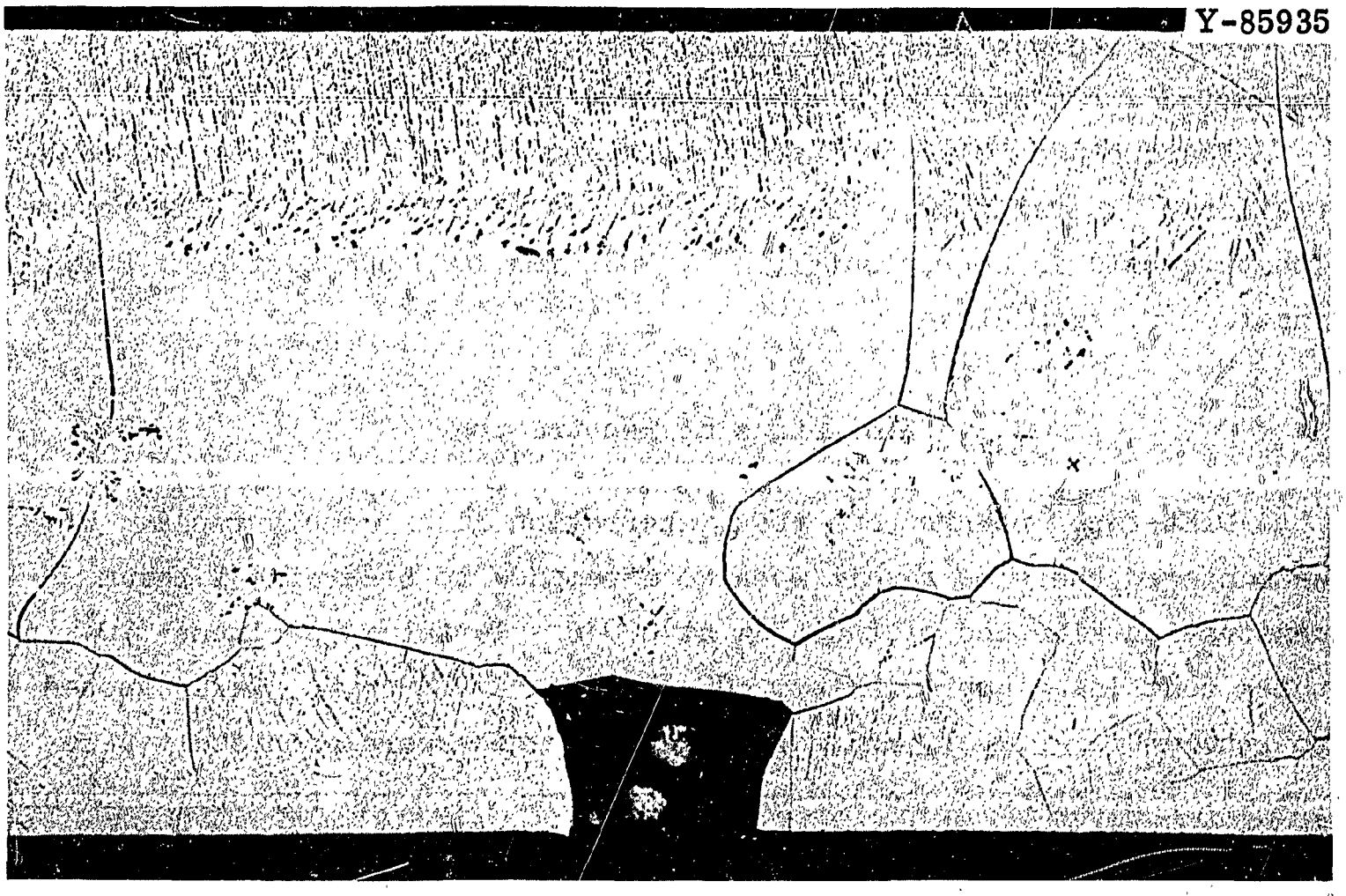

Fig. 6. Niobium That Contained 2200 ppm O and Was Exposed to Lithium for 500 hr at 600°C. Note how the grain-boundary attack has caused one grain to fall out of the specimen. 100×. Etchant: $HF-HNO_3-H_2SO_4-H_2O$.

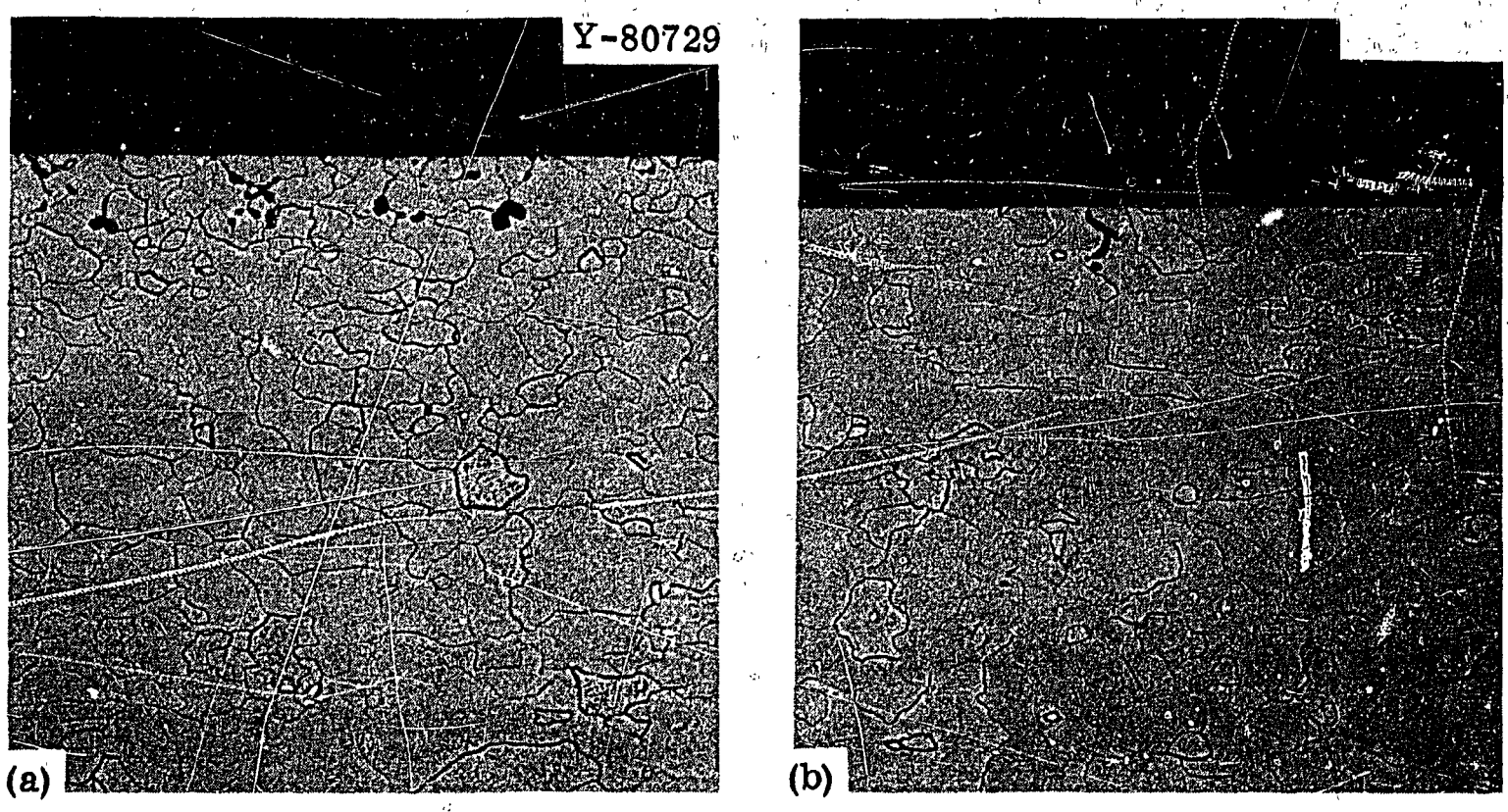

Fig. 7. Tantalum Exposed to Potassium for 100 hr at 800°C. 100×. Etchant: $H_2O-HNO_3-NH_4HF$. (a) Initially 1200 ppm O, (b) 700 ppm O.

no penetration was detected, and little attack [similar to Fig. 7(b)] was noted for a specimen containing 1000 ppm O.

We conclude that the threshold oxygen concentration for the penetration of tantalum by potassium increases with increasing temperature. The threshold is approximately 500, 700, and 1000 ppm O at 600, 800, and 1000°C, respectively.

Kinetics of Penetration

DiStefano[5] pointed out that penetration is extremely rapid. We encountered the same result when we attempted to study the lithium penetration kinetics of tantalum at 600°C. Tantalum specimens 0.04 in. thick containing approximately 600, 1200, and 3000 ppm O were exposed to lithium for 0.5, 1, and 2 hr. All specimens were completely penetrated; Fig. 8 shows the low-oxygen specimen that was exposed to lithium for 0.5 hr.

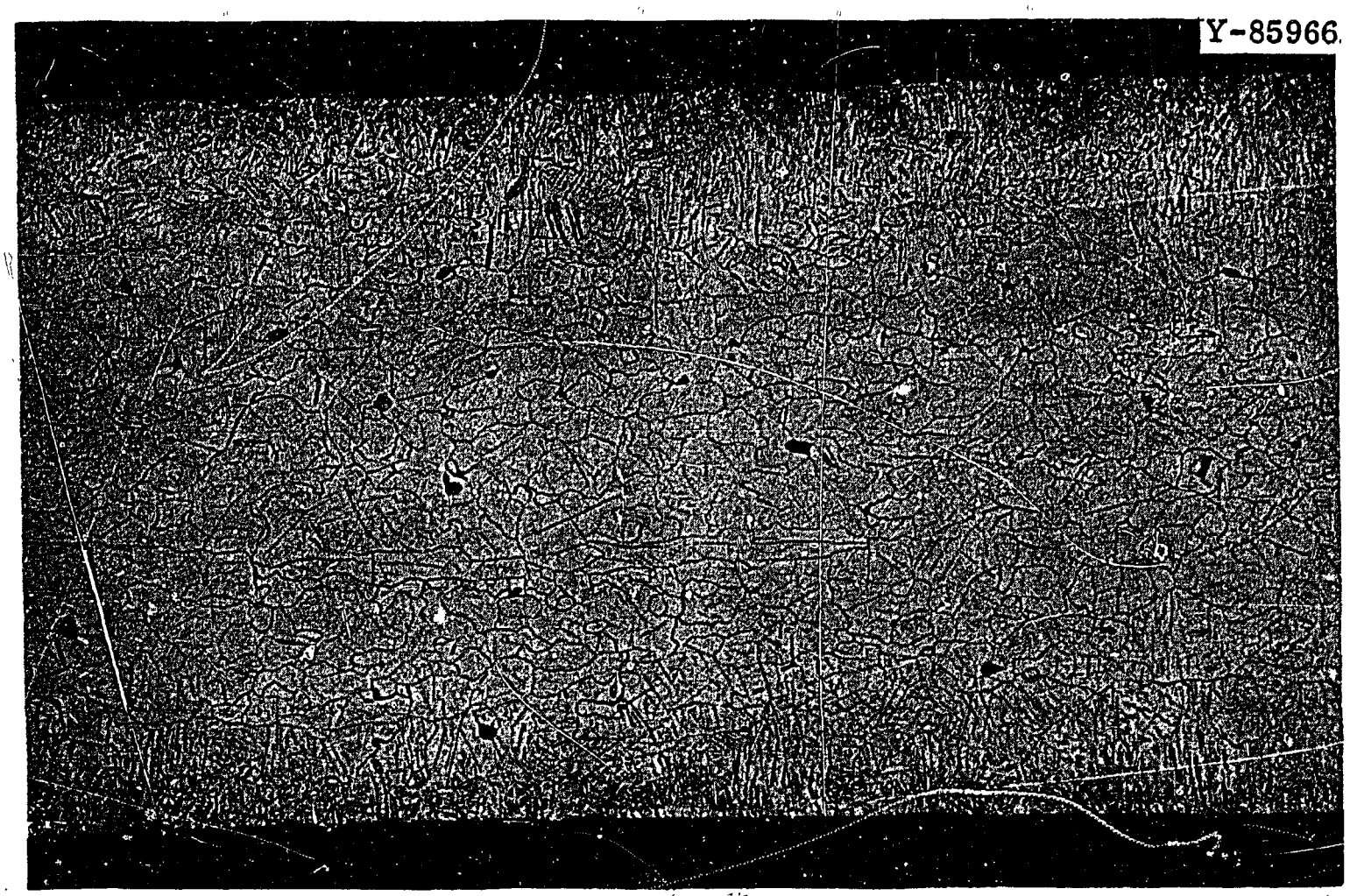

Fig. 8. Tantalum That Contained 600 ppm O and Was Exposed to Lithium for 0.5 hr at 600°C. 100×. Etchant: H_2O-HNO_3-NH_4HF.

At present we are attempting to study the penetration kinetics at 250°C, where the penetration is slower.

General Observations

Tantalum and niobium exposed to any of the alkali metals for 100 hr or more showed a loss of oxygen during test. Table 2 gives the changes noted at 600, 800, and 1000°C for the tantalum specimens penetrated by potassium. The oxygen concentrations at 800 and 1000°C decreased to a

Table 2. Change in the Oxygen Concentration of Tantalum Exposed to Potassium

Temperature (°C)	Exposure (hr)	Oxygen Concentration, ppm	
		Before	After
600	500	600	170
800	100	700	34
800	100	1200	36
1000	50	600	39
1000	50	1000	53
1000	50	1600	23

level near that found in undoped specimens exposed for comparable times and temperatures. Since only intergranular penetration occurred at these higher temperatures, only a very small fraction of the total oxygen is tied up in a corrosion product. Furthermore, some of the corrosion product may be lost when the alkali metal adhering to the specimen after test is dissolved in alcohol.

All attempts at identifying the corrosion product were unsuccessful. Metallographic examination of penetrated specimens generally show the attacked regions as holes, indicating that the corrosion product had dissolved during polishing. When a penetrated specimen was fractured and examined with the scanning electron microscope, a second phase, presumably a corrosion product, was observed on grain boundaries, as

shown in Fig. 9. The specimen fracture followed the morphology of the corrosion product. When the specimen shown in Fig. 8 was fractured and examined under the scanning electron microscope, two distinct regions were visible. The region immediately adjacent to the surface fractured transgranularly and corresponded to the region of extensive transgranular attack. In the center of the specimen, intergranular fracture occurred and corresponded to the region where attack was primarily along grain boundaries.

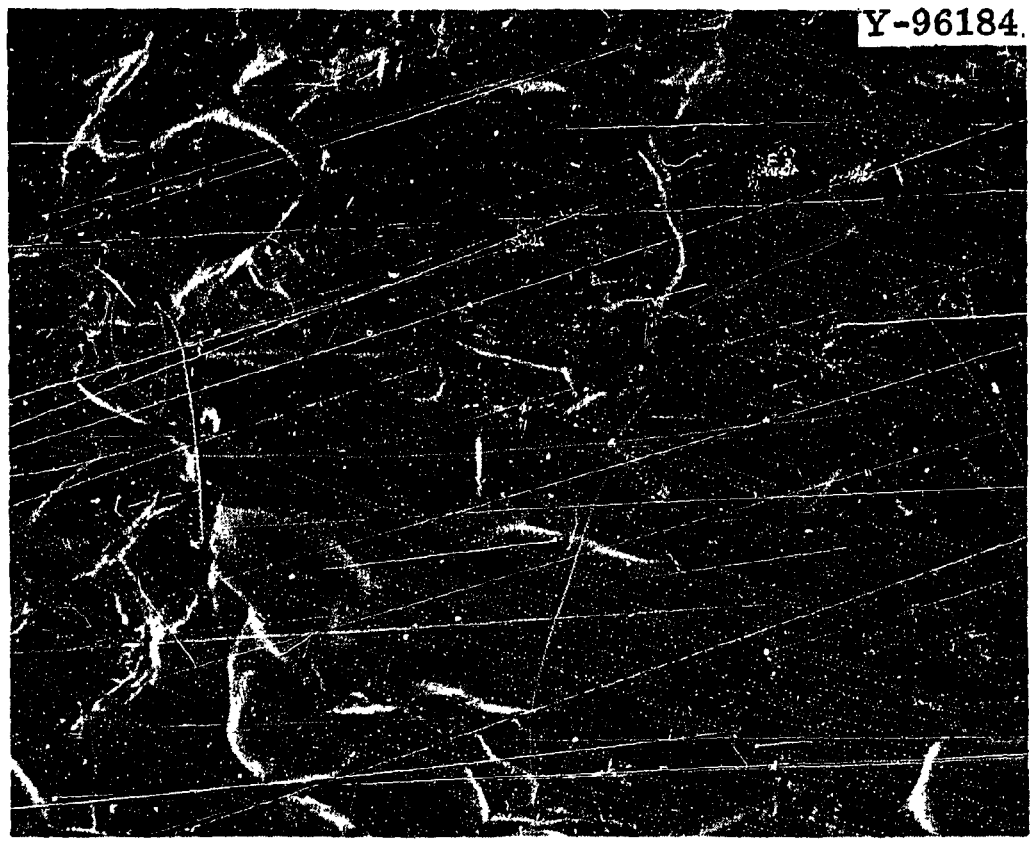

Fig. 9. Fracture Surface From Interior of Specimen Shown in Fig. 8. Note that the grain surfaces appear to contain a second phase. 850×.

DISCUSSION

General

If we assume that alkali metal penetration occurs by the formation of a corrosion product, several of the experimental observations are consistent with classical nucleation theory. The start of penetration requires a nucleation step and thus requires the formation of a critical nucleus of the compound making up the corrosion product. As with all

nucleation processes, supersaturation will be required — hence the threshold oxygen concentration. Surface energy and strain energy considerations favor nucleation on grain boundaries and thus account for the lower threshold levels for intergranular attack.

In general the standard free energy of formation for oxides becomes more negative with decreasing temperature. The oxygen concentration necessary to form a critical nucleus should therefore decrease with decreasing temperature, as observed. DiStefano,[12] in some low-temperature experiments, noted an incubation period before attack starts; such an observation is again in accord with a nucleation step.

Table 1 shows that the threshold for tantalum is roughly one-half that for niobium. Thermodynamically, the threshold oxygen concentration should be considered in terms of a threshold oxygen activity. The oxygen solubility in niobium[13] is about twice that of tantalum,[14] and therefore, if the oxygen-saturated solutions are taken as the standard state and if Henry's law applies to saturation, the threshold oxygen activities are nearly equal in tantalum and niobium.

Penetration Model

Any penetration model must explain the effects of time and oxygen concentration on penetration rate. Table 3, taken from DiStefano,[5] shows the effect of time on the penetration of niobium by lithium. Of interest are the tests above 260°C where penetration depth did not increase significantly between 1 and 100 hr. This occurred for the specimens with 1000 ppm O at 538 and 816°C. Note also how final penetration depth and penetration depth in the first hour of exposure increased with oxygen concentration.

At elevated temperatures, DiStefano[5] attributed the cessation of penetration to the removal of oxygen from the niobium by the lithium. He showed with diffusion calculations that after 1 hr at 816°C the oxygen concentration 0.005 in. below the external surface of a specimen that initially contained 1000 ppm O was below the threshold oxygen concentration. This was not the case for specimens initially containing 1700 ppm O or more, which were completely penetrated by the lithium at 816°C.

Table 3. Effect of Time on the Depth of Penetration of Oxygen-Contaminated Niobium by Lithium, Taken from DiStefano[5]

Oxygen Concentration (ppm)	Type of Specimen	Temperature (°C)	Time (hr)	Depth of Attack (in.)
1000	Polycrystalline	260	1	0.007
1000	Polycrystalline	260	100	0.016
1000	Polycrystalline	538	1	0.009
1000	Polycrystalline	538	100	0.012
1000	Single crystal	816	1	0.003
1000	Single crystal	816	250	0.003
1700	Single crystal	816	0.1	0.003
1700	Single crystal	816	1	0.005
1700	Single crystal	816	100	0.030[a]
1200	Single crystal	538	0.5	0.006
1200	Single crystal	538	30	0.013
4475	Single crystal	816	0.1	0.012
4475	Single crystal	816	1	0.033[a]

[a]Complete.

Oxygen depletion, however, does not explain the lower temperature test results. For example, using Ang's[15] value for the oxygen diffusion coefficient in niobium, we have calculated that the oxygen concentration 0.012 in. below the surface should still be 90% of its original value even after 100 hr at 538°C; this would be well above the threshold oxygen concentration.

Diffusion Model

Brehm et al.[6] were the only investigators that attempted to determine the attack mechanism. They studied the lithium penetration of oriented, oxygen-doped (700, 1500, and 2400 ppm O) niobium bicrystals at 800, 900, and 1000°C. The depth of grain boundary penetration varied as $(\text{time})^{1/2}$ with an activation energy of 70 kcal/mole. These authors, like DiStefano, assumed that penetration results from the formation of

an unidentified lithium-oxygen-niobium compound that they observed visually on the surface of fractured specimens.

Brehm et al. proposed a model that assumes that lithium diffuses into the grain boundary and reacts with oxygen and niobium to form the corrosion product. Lithium diffusion to the reaction front is assumed the rate-limiting step. Since the activation energy for volume diffusion is over 100 kcal/mole, the authors concluded that grain-boundary diffusion is rate limiting.

Mathematical analyses of this problem are available,[16,17] and Brehm et al. chose the Darken analysis[16] and attempted to get a qualitative fit with their data. Wagner[17] has derived equations similar to those of Darken[16] for a reaction zone moving as $t^{1/2}$ and has shown that when

$$D_O/D_{Li} \ll N_{Li}^{(s)}/N_O \ll 1 , \tag{1}$$

$$X = \left(2D_{Li}N_{Li}^{(s)}t/\upsilon N_O\right)^{1/2} , \tag{2}$$

where

X = distance from specimen surface to the penetration front,

t = time,

D_O = oxygen diffusion coefficient in niobium,

$N_{Li}^{(s)}$ = lithium concentration in niobium at the lithium-niobium interface,

N_O = initial oxygen concentration of niobium,

υ = ratio of lithium to oxygen in the corrosion product.

As seen in Eq. (2), the rate of penetration (dX/dt) should decrease as N_O increases. Experimentally Brehm et al.[6] found an increase in penetration rate with N_O. Since the model predicts that the rate of penetration is directly proportional to the lithium concentration at the niobium surface, $N_{Li}^{(s)}$, they proposed that the discrepancy was resolved if $N_{Li}^{(s)}$ increased with oxygen concentration faster than the oxygen concentration increases. However, such an explanation does not appear justified, since the niobium specimens lose oxygen to the lithium.

Hence the oxygen concentration at the niobium surface is quickly reduced to that in equilibrium with the liquid lithium (essentially zero).

Equation (2) can be used to calculate X only when the conditions of Eq. (1) are met. Physically Eq. (1) means that the oxygen reacts in place[18] (i.e., the flux of lithium into the niobium is very much greater than that of oxygen out). As we have seen, at 538°C there is essentially no oxygen diffusion relative to the advance of the penetration front, and Eq. (2) should apply if the model is valid.

Equation (2) can be applied directly only if we know $N_{Li}^{(s)}$ and D_{Li}. All indications are that the lithium solubility in niobium is extremely small and even at relatively high temperatures is probably less than 100 ppm. No data are available on D_{Li}. If we assume that the lithium concentration at the niobium surface is 100 ppm, we can use Eq. (2) along with the data of Table 3 to calculate D_{Li}. Then using this diffusion coefficient we can calculate the time for complete penetration. For the specimen penetrated 0.009 in. in 1 hr at 538°C (assume $\upsilon = 1$), D_{Li} is calculated to be 3.1×10^{-7} cm^2/sec. This value is much larger than any known diffusion coefficient for substitutional diffusion – even grain boundary diffusion at 538°C. If we now use this value for D_{Li}, Eq. (2) predicts that the specimen should be completely penetrated (0.02 in.) in 5 hr. As seen in Table 3, the specimen is not completely penetrated in 100 hr. Hence the diffusion model fails on two counts. Qualitatively the observed effect of $N_O^{(s)}$ is opposite to that predicted, and the apparent cessation of penetration at lower temperatures is not accounted for.

Proposed Model

As an alternative to the diffusion model, we tentatively propose that alkali metal attack occurs by a wedging mechanism. Wedging results from the formation of corrosion products having a larger volume than the metal from which they form. Nielsen[19] proposed that such a mechanism occurs during the stress corrosion of austenitic stainless steels, and Pickering et al.[20] showed that cracks could be propagated by corrosion

products in the absence of any externally applied stress. The mechanism is qualitative and has not yielded to mathematical analysis.

The conditions for wedging require a corrosion product larger in volume than the metal from which it formed. Litman[9] noted that the corrosion products that formed when niobium containing 2400 ppm O was exposed to potassium at 815°C were of lower density than the matrix. When the external surface was examined, metallic protuberances were observed, as shown in Fig. 10. These markings were found only when the niobium initially contained more than 1000 ppm O. When the specimens were sectioned the position of the subsurface corrosion products often matched the locations of the surface protuberances, as shown in Fig. 11. We also observed this "bulging" effect in tantalum penetrated by potassium and sodium.

Fig. 10. Protuberances on the Surface of a Niobium Specimen That Contained 2400 ppm O and Was Exposed to Potassium for 100 hr at 815°C. 20×. [Ref: A. P. Litman, The Effect of Oxygen on the Corrosion of Niobium by Liquid Potassium, ORNL-3751 (July 1965).]

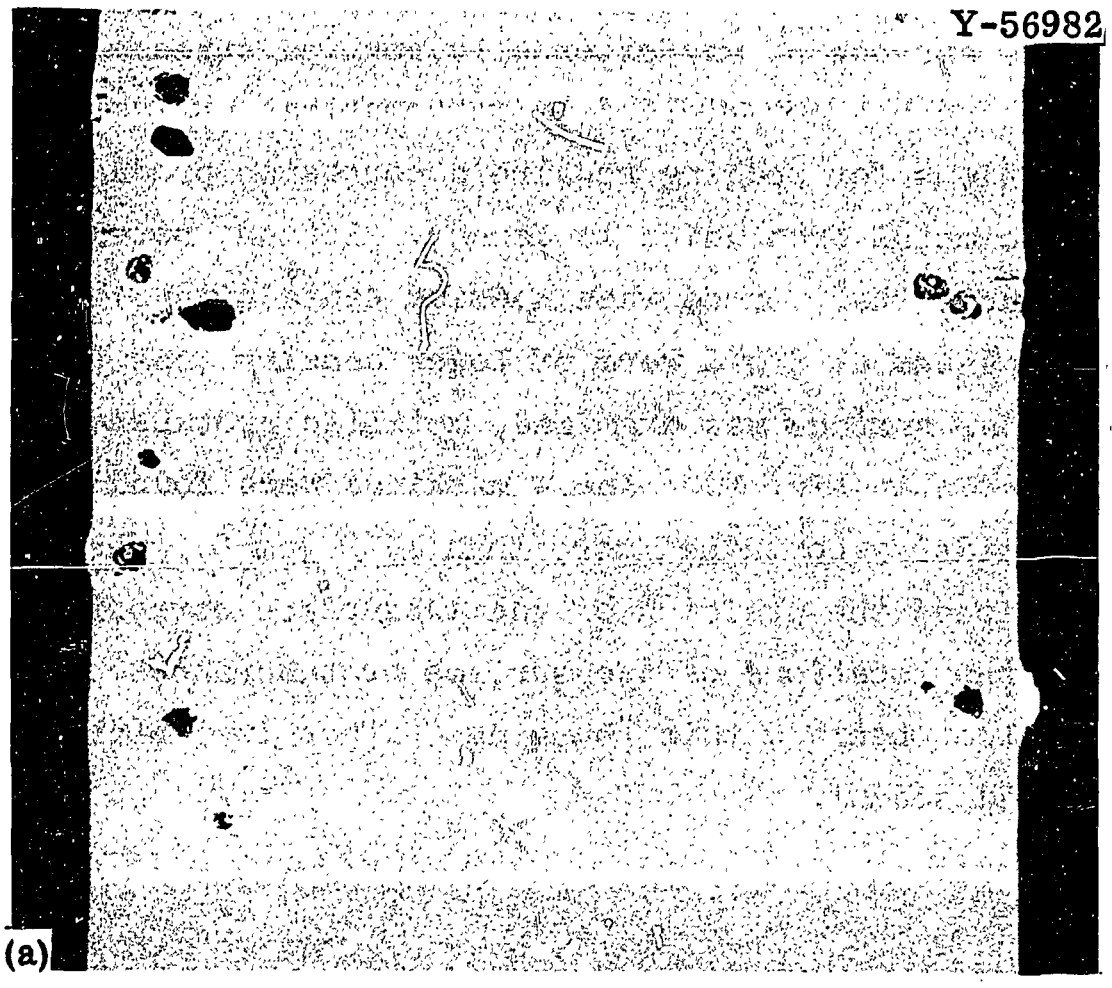

Fig. 11. Cross Section of Specimen Shown in Fig. 10 Showing How the Protuberences Were Formed. Unetched. (a) 100×. (b) 500×. [Ref: A. P. Litman, The Effect of Oxygen on the Corrosion of Niobium by Liquid Potassium, ORNL-3751 (July 1965).]

Bulging is only observed in conjunction with attack that shows the large "heads" at the end of the penetration, although not all attack showing "heads" exhibits bulging. The distance of the "head" from the external surface probably determines whether bulging occurs or not.

Following Pickering et al.[20] we propose that the pressure of the larger volume of products that forms wedges open the material in front of it to form a crack. Liquid metal is drawn to the crack tip by either or both of the following mechanisms: (1) the newly formed cavity represents a low-pressure region into which the liquid metal is forced; (2) the liquid metal is attracted to the crack tip by capillary action. Pickering et al.[20] gave a derivation by Hirth for the average velocity of the liquid as it flows through the penetrated region to the crack tip by capillary action as

$$v \cong \frac{\delta \gamma_{v\ell} \cos \theta}{4\eta x} , \qquad (3)$$

where

x = distance from the specimen surface,

δ = one-half of crack width wedged open by the corrosion product,

η = coefficient of viscosity,

$\gamma_{v\ell}$ = surface tension of liquid,

θ = contact angle of the liquid with the solid.

Corrosion-product wedging can qualitatively account for the observations on liquid metal attack. The penetration rate increases with increasing oxygen concentration of the refractory metal because greater amounts of corrosion products are formed, which lead to higher stresses, and thus larger amounts of liquid are transferred to the reaction front. That is, the higher stresses developed by the larger amount of products lead to a larger δ and thus a larger v. At lower oxygen concentrations, δ decreases and the rate at which liquid reaches the front eventually decreases to the point where penetration essentially ceases.

The corrosion heads found on the ends of some penetrations may result when the liquid transfer to the reaction front is rate controlling. These heads are found only at higher temperatures (at least 600°C), where oxygen diffusion becomes important. When penetration slows or stops because v decreases, oxygen can diffuse from the immediate surroundings to the reaction front and react locally with the available liquid (i.e., oxygen diffuses to the reaction front at a rate greater than or equal to the rate at which liquid arrives at the reaction front). Reaction ceases when oxygen is depleted from the specimen.

The wedging mechanism is also consistent with the observation of a maximum transgranular penetration depth with temperature.[5] At elevated temperatures the decrease is explained by oxygen depletion from the specimen, as discussed in the preceding section. At low temperatures, where oxygen diffusion is slow, penetration ceases because v approaches zero. The velocity is a function of temperature through η and θ. The viscosity[21] and the contact angle[22] decrease with increasing temperature, leading to an increase in v and thus increased penetration.

ACKNOWLEDGMENTS

Appreciation is expressed to J. L. Griffith, Jr., for carrying out the experiments, to J. R. DiStefano, J. H. DeVan, and C. E. Sessions for helpful discussions throughout the course of this work, and to Sharon Woods for the preparation of the manuscript.

REFERENCES

1. R. L. Klueh, "The Effect of Oxygen in Sodium on the Compatibility of Sodium and Niobium," pp. 171–176 in Proceedings of the International Conference on Sodium Technology and Large Fast Reactor Design, November 7–9, 1968, ANL-7520, Part I.
2. R. L. Klueh, "The Effect of Oxygen on the Compatibility of Niobium with Potassium," Corrosion 25, 416–422 (1969).

3. E. E. Hoffman, The Effect of Oxygen and Nitrogen on the Corrosion Resistance of Columbium to Lithium at Elevated Temperatures, ORNL-2675 (Jan. 16, 1959).
4. M. S. Freed and K. J. Kelly, Corrosion of Columbium Base and Other Structural Alloys in High Temperature Lithium, PWAC-355 (June 1961).
5. J. R. DiStefano, Corrosion of Refractory Metals by Lithium, ORNL-3551 (March 1964).
6. W. F. Brehm, Jr., J. L. Gregg, and Che-Yu Li, "Grain Boundary Penetration of Niobium (Columbium) by Lithium," Trans. Met. Soc. AIME 242, 1205–1210 (1968).
7. S. C. Weaver, private communication.
8. R. W. Harrison, Corrosion of Oxygen Contaminated Tantalum in NaK, Topical Report 1, GESP-138 (January 1969).
9. A. P. Litman, The Effect of Oxygen on the Corrosion of Niobium by Liquid Potassium, ORNL-3751 (July 1965).
10. C. W. Hickam, Jr., "Corrosion Product of the Tantalum-Interstitial Oxygen-Potassium System at 1800°F (982°C)," J. Less-Common Metals 14, 315–322 (1968).
11. C. E. Sessions, unpublished research.
12. J. R. DiStefano, private communication.
13. E. Gebhardt and R. Rothenbacher, "Investigations in the System Niobium-Oxygen II. Solution of Oxygen in Niobium and Precipitation of Oxides from Supersaturated Solid Solutions," Z. Metallk. 54, 623–630 (1963).
14. E. Gebhardt and H. D. Seghezzi, "Investigations in the System Tantalum Oxygen II. Reactions and Equilibria Between Solid Solution and Oxide Phases," Z. Metallk. 50, 521–527 (1959).
15. C. Y. Ang, "Activation Energies and Diffusion Coefficients of Oxygen and Nitrogen in Niobium and Tantalum," Acta Met. 1, 123–125 (1953).
16. L. S. Darken, "Diffusion in Metal Accompanied by Phase Change," Trans. AIME 150, 157–171 (1942).
17. C. Wagner, "Reaction Types in the Oxidation of Alloys," Z. Elektrochem. 63, 772–782 (1959).

18. R. A. Rapp, "Kinetics, Microstructure, and Mechanism of Internal Oxidation – Its Effect and Prevention in High Temperature Alloy Oxidation," Corrosion 21, 382–401 (1965).

19. N. A. Nielsen, Proceedings of Symposium on Physical Metallurgy of Stress Corrosion Fracture (T. N. Rhodin, editor), Interscience Publishers, New York, 1959, p. 121.

20. H. W. Pickering, F. H. Beck, and M. G. Fontana, "Wedging Action of Solid Corrosion Products During Stress Corrosion of Austenitic Stainless Steels," Corrosion 18, 230t–239t (1962).

21. W. J. Moore, Physical Chemistry, 3rd ed., Prentice Hall, Englewood Cliffs, N. J., 1962, p. 723.

22. J. W. Taylor, Progr. Nucl. Energy, Ser. V. Metallurgy and Fuels. 2, ed. by H. M. Finniston and J. P. Howe, Pergamon Press, London, 1959, p. 398.